Upper critical fields and superconducting anisotropy of $K_{0.70}Fe_{1.55}Se_{1.01}S_{0.99}$ and $K_{0.76}Fe_{1.61}Se_{0.96}S_{1.04}$ single crystals

Hechang Lei and C. Petrovic Condensed Matter Physics and Materials Science Department, Brookhaven National Laboratory, Upton, NY 11973, USA (Dated: November 17, 2018)

We have investigated temperature and angular dependence of resistivity of $K_{0.70(7)}Fe_{1.55(7)}Se_{1.01(2)}S_{0.99(2)}$ and $K_{0.76(5)}Fe_{1.61(5)}Se_{0.96(4)}S_{1.04(5)}$ single crystals. The upper critical fields $\mu_0H_{c2}(T)$ for both field directions decrease with the increase in S content. On the other hand, the angle-dependent magnetoresistivity for both compounds can be scaled onto one curve using the anisotropic Ginzburg-Landau theory. The obtained anisotropy of $\mu_0H_{c2}(T)$ increases with S content, implying that S doping might decrease the dimensionality of certain Fermi surface parts, leading to stronger two dimensional character.

PACS numbers: 74.25.Op, 74.70.Xa, 74.25.F-

I. INTRODUCTION

Iron-based superconductors have stimulated intense activity after the discovery of LaFeAsO_{1-x} F_x with T_c $= 26 \text{ K (FeAs-1111 type)}^{1}$. Since then, the family of iron-based superconductors has been gradually expanded to include AFe₂As₂ (A = alkaline or alkalineearth metals, FeAs-122 type)², LiFeAs (FeAs-111 type)³. and α -PbO type FeCh (Ch = S, Se, or Te, FeSe-11 type)⁴. Even though these compounds share similar structural features and possible same pairing s± symmetry⁵, the superconducting properties exhibit pronounced difference. Among these, the diversity of temperature dependence of the upper critical field $\mu_0 H_{c2}(T)$ attracts much interest since it provides valuable information on the fundamental superconducting properties. These include coherence length, anisotropy, details of underlying electronic structure, dimensionality of superconductivity as well as insights into the pair-breaking mechanism. For FeAs-1111 type and FeAs-122 type superconductors, the $\mu_0 H_{c2}(T)$ can be described using a two-band $model^{6-8}$. However, for FeSe-11 type and arsenic-deficient FeAs-1111 type compounds, the $\mu_0 H_{c2}(T)$ exhibits Pauli-limiting behavior and satisfies the single-band Werthamer-Helfand-Hohenberg (WHH) theory with strong spin-paramagnetic effect and spinorbital interaction 9-12.

Very recently, new family of iron-based superconductors $A_xFe_{2-y}Se_2$ (A = K, Rb, Cs, and Tl, AFeSe-122 type) with maximum $T_c \approx 33$ K has been reported ¹³- ¹⁹. Superconductivity in AFeSe-122 materials is in proximity to an antiferromagnetic (AFM) semiconducting state ^{19,20}. This is different from other iron based superconductors, which are usually close to spin density wave (SDW) instability, and similar to cuprates where parent compounds are AFM Mott insulators. Therefore, it is of interest to study whether this kind of difference will lead to different behavior of $\mu_0 H_{c2}(T)$. Preliminary $\mu_0 H_{c2,c}(T)$ and $\mu_0 H_{c2,ab}(T)$ of AFeSe-122 estimated within simplified WHH model are about 40-70 T and 120-220 T, respectively, giving the anisotropy of

 $\mu_0 H_{c2}(0)$ about 3-4^{14,15,17,20}. However, the $\mu_0 H_{c2}(T)$ of $K_x Fe_{2-y} Se_2$ measured up to 60 T deviates from the WHH model and is similar to FeAs-122 materials²¹.

Insulating $K_xFe_{2-y}S_2$ is isostructural with $K_xFe_{2-y}Se_2^{22}$. It is of interest to study changes of $\mu_0H_{c2}(T)$ in AFeSe-122 with S doping. In this work, we report the upper critical field anisotropy of $K_{0.70(7)}Fe_{1.55(7)}Se_{1.01(2)}S_{0.99(2)}$ and $K_{0.76(5)}Fe_{1.61(5)}Se_{0.96(4)}S_{1.04(5)}$ single crystals. We show that both $\mu_0H_{c2,c}(T)$ and $\mu_0H_{c2,ab}(T)$ decrease with S doping but the anisotropy of $\mu_0H_{c2}(T)$ is larger than in $K_xFe_{2-y}Se_2$.

II. EXPERIMENT

The details of crystal growth and structure characterization are reported elsewhere in detail^{22,23}. stoichiometry determined The average by dispersive X-ray spectroscopy (EDX) ergy K:Fe:Se:S 0.70(7):1.55(7):1.01(2):0.99(2)and 0.76(5):1.61(5):0.96(4):1.04(5) for S-99 and S-104, respectively. The in-plane resistivity $\rho_{ab}(T)$ was measured using a four-probe configuration on rectangularly shaped and polished single crystals with current flowing in the ab-plane of tetragonal structure. Thin Pt wires were attached to electrical contacts made of Epotek H20E silver epoxy. Sample dimensions were measured with an optical microscope Nikon SMZ-800 with 10 μ m resolution. Electrical transport and magnetization measurements were carried out in a Quantum Design PPMS-9 and MPMS-XL5.

III. RESULTS AND DISCUSSION

Fig. 1(a) shows the temperature dependence of inplane resistivity $\rho_{ab}(T)$ at zero field from 10 K to 300 K. Similar to $K_x Fe_{2-y} Se_2$, both S-99 and S-104 exhibit semiconducting behavior at high temperature and then cross over to metallic behavior. With further decrease in

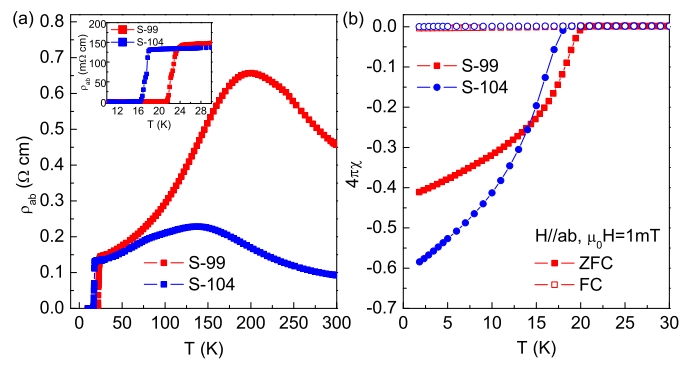


FIG. 1. (a) Temperature dependence of the in-plane resistivity $\rho_{ab}(T)$ of S-99 and S-104 at zero field. Inset shows resistivity near superconducting transition temperature. (b) Temperature dependence of dc magnetic susceptibility of S-99 and S-104 with ZFC and FC.

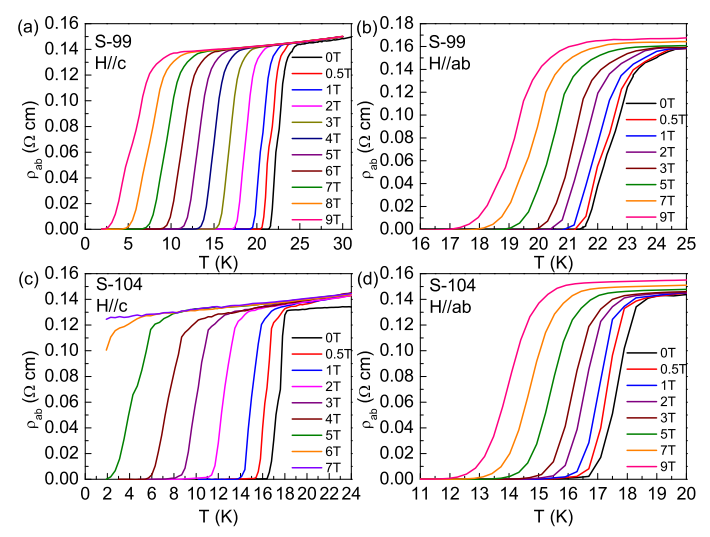


FIG. 2. Temperature dependence of the resistivity $\rho_{ab}(T)$ in magnetic fields for (a) H||ab and (b) H||c of S-99 and (c) H||ab and (d) H||c of S-104.

temperature, there are sharp superconducting transitions with $T_{c,onset}=23.5(1)$ K and 18.0(2) K for S-99 and S-104, respectively. It should be noted that the large shift of T_c in our crystals can not be explained by the small variations of K and Fe contents^{19,20}. Fig. 1(b) shows the temperature dependence of the dc magnetic susceptibility of S-99 and S-104 for $\mu_0 H=1$ mT along the abplane. The zero-field-cooling (ZFC) susceptibilities show that the superconducting shielding emerges at about 18.0 K and 20.4 K for S-99 and S-104, consistent with the T_c obtained from resistivity measurement. The superconducting volume fractions estimated from the ZFC magnetization at 1.8 K are about 0.41 and 0.58 for S-99 and S-104, respectively, indicating substantial, albeit still filamentary superconducting volume fraction.

Fig. 2 shows temperature dependent resistivity of $\rho_{ab}(T)$ of S-99 and S-104 in magnetic fields up to 9 T for H||c and H||ab. With increasing magnetic fields, the superconducting transitions shift to lower temperature

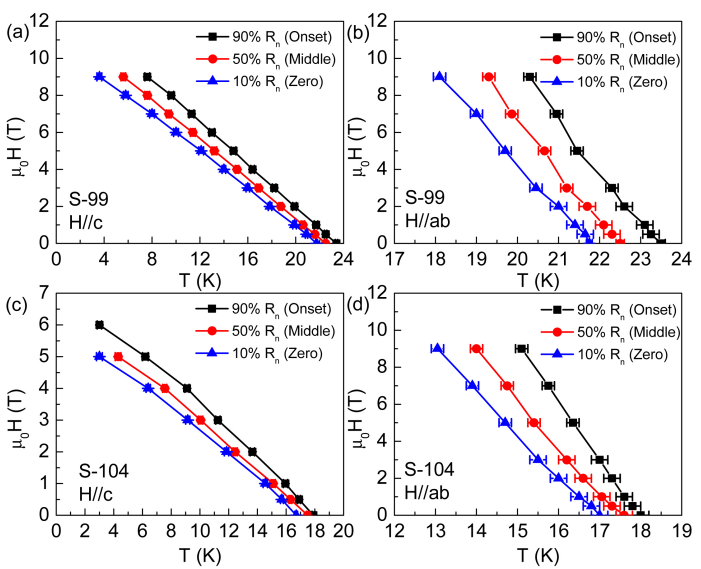


FIG. 3. Temperature dependence of the resistive upper critical field $\mu_0 H_{c2}(T)$ of S-99 for (a) H||ab and (b) H||c, and of S-104 for (c) H||ab and (d) H||c.

gradually and transition widths become broader. This trend is more obvious for H||c than for H||ab. is similar to Fe(Te,Se) and Fe(Te,S) single crystals^{9,10}. When compared to pronounced broadening of resistivity in magnetic field in FeAs-1111 compounds for $H\|c^{24,25}$. the broadening of resistivity in AFeSe-122 materials is far smaller for both field directions, similar to the FeAs-122 and FeSe-11 compounds^{9,10,26,27}. This indicates that the vortex-liquid state region should be narrower in AFeSe-It should be noted that this narrow transition widths could also have contribution from the normal state parts of samples. On the other hand, the superconductivity in S-99 and S-104 is more sensitive to the field for H||c when compared to undoped $K_x Fe_{2-u} Se_2$. The $T_{c,onset}$ of S-99 has shifted to 7.6(2) K at $\mu_0 H =$ 9 T, whereas for S-104, the superconductivity has been suppressed completely above 1.9 K even at $\mu_0 H = 7$ T. This indicates that the $\mu_0 H_{c2,c}(T)$ of S-99 and S-104 are much lower than in $K_x \text{Fe}_{2-y} \text{Se}_2$.

Fig. 3 presents the temperature dependence of the resistive upper critical fields $\mu_0 H_{c2}(T)$ of S-99 and S-104 determined from resistivity drops to 90% (Onset), 50% (Middle) and 10% (Zero) of the normal state resistivity $\rho_{n,ab}(T,H)$ for both field directions. The normal-state resistivity $\rho_{n,ab}(T,H)$ was determined by linearly extrapolating the normal-state behavior above the onset of superconductivity in $\rho_{ab}(T,H)$ curves. It can be seen that the $\mu_0 H_{c2}(T)$ for H||c is much smaller than that for H||ab. Hence the low field anisotropy of $\mu_0 H_{c2}(T)$ for both of S-99 and S-104 is large, similar to $K_x Fe_{2-y} Se_2^{14,15,20}$. On the other hand, the low field positive curvature of $\mu_0 H_{c2,ab}(T)$ shows a slight positive curvature which may be due to a crossover from three dimensions (3D) to two dimensions (2D)²⁸.

According to the conventional single-band WHH the-

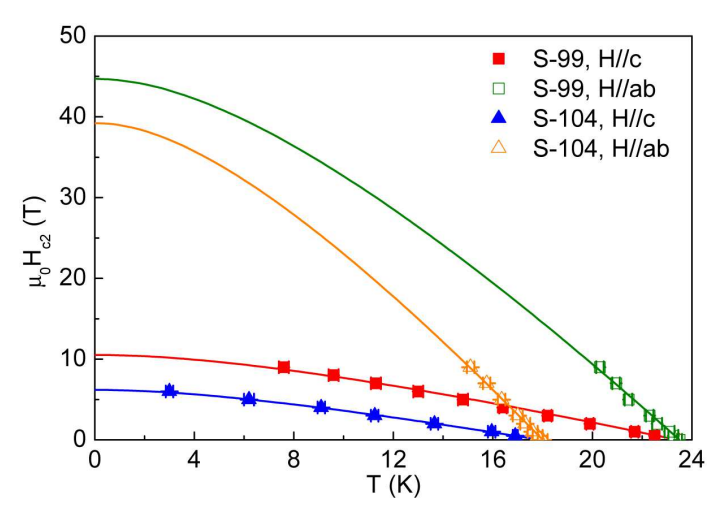


FIG. 4. Fits to $\mu_0 H_{c2,c}(T)$ and $\mu_0 H_{c2,ab}(T)$ using the simplified WHH theory for (a) S-99 and (b) S-104. The $\mu_0 H_{c2,c}(T)$ and $\mu_0 H_{c2,ab}(T)$ of S-99 and S-104 are determined from 90% of $\rho_{n,b}(T,H)$.

ory which describes the orbital limited upper critical field of dirty type-II superconductors²⁹, the $\mu_0 H_{c2}$ can be described by

$$\ln \frac{1}{t} = \psi(\frac{1}{2} + \frac{\bar{h}}{2t}) - \psi(\frac{1}{2}) \tag{1}$$

where $t = T/T_c$, ψ is a digamma function and

$$\frac{1}{h} = \frac{4H_{c2}}{\pi^2 T_c (-dH_{c2}/dT)_{T=T_c}}$$
(2)

Using the measured $T_{c,onset}$ and setting the slopes of $\mu_0 H_{c2}(T)$ near $T_{c,onset}(\mu_0 H = 0)$, $-d(\mu_0 H_{c2})/dT|_{T=T_c}$, as free parameters, the $\mu_0 H_{c2}(0)$ of S-99 and S-104 along both field directions can be obtained using the simplified WHH model. As shown in Table 1, the fitted $-d(\mu_0 H_{c2})/dT|_{T=T_c}$ are much smaller than in $K_x \text{Fe}_{2-y} \text{Se}_2$, which are about 2-3 T/K for H||c and 6-10 T/K for H||ab^{15,20}. Correspondingly, the $\mu_0 H_{c2}(0)$ for both field directions are also much smaller than in $K_x \text{Fe}_{2-y} \text{Se}_2^{14,15,20,21}$. From the $\mu_0 H_{c2}(0)$, zero-temperature coherence length $\xi(0)$ can be estimated with Ginzburg-Landau (GL) formula $\mu_0 H_{c2,c}(0) = \Phi_0/[2\pi \xi_{ab}^2(0)]$, and $\mu_0 H_{c2,ab}(0) = \Phi_0 / [2\pi \xi_{ab}(0)\xi_c(0)]$ where $\Phi_0 = 2.07 \times 10^{-15}$ The zero-temperature anisotropy $(\Gamma(0))$ = $H_{c2,ab}(0)/H_{c2,c}(0)$ obtained from WHH fits for S-99 and S-104 is 4.26 and 5.56, respectively. The $\Gamma(0)$ of S-104 is larger than that of S-99, and both are larger than in $K_x \text{Fe}_{2-y} \text{Se}_2^{14,15,20}$. All obtained parameters are listed in Table 1 and the fitting results are show in fig.

It should be noted that the $\mu_0 H_{c2,c}(T)$ of S-99 can be fitted linearly with slightly lower fitting error when

compared to simplified WHH theory, whereas the fitting quality using simplified WHH theory is much better than linear function for S-104. This linear behavior has also been observed in $K_x \text{Fe}_{2-y} \text{Se}_2^{21}$. It implies that S doping could change the temperature dependence of $\mu_0 H_{c2,c}(T)$ possibly due to the changes of band structure. Agreement with simplified WHH theory with temperature far below T_c for H||c implies that for S-99 the orbital effect should be the dominant pairbreaking mechanism and spin-paramagnetic effect and spin-orbital interaction could be negligible when the magnetic field is applied along c axis. This is different from FeSe-11 materials where the $\mu_0 H_{c2,c}(T)$ exhibits Paulilimiting behavior and strong spin-orbital interaction has to be considered^{9,10}. Pauli limiting field is $\mu_0 H_p(0) =$ $1.86T_c(1 + \lambda_{e-ph})^{1/2}$, where λ_{e-ph} is electron-phonon coupling parameter³⁰. Using the typical value for weakcoupling BCS superconductors $(\lambda_{e-ph} = 0.5)^{31}$, we ob $tain \mu_0 H_n(0) = 53.5 \text{ T} \text{ and } 41.0 \text{ T} \text{ for S-99 and S-104},$ respectively. Both values are larger than extrapolated $\mu_0 H_{c2,c}(0)$ using simplified WHH theory for S-99 and S-104 and also larger than the value determined from linear extrapolation $(\mu_0 H_{c2,c}(0) = 13.47(4) \text{ T})$ for S-99. On the other hand, the $\mu_0 H_{c2,c}(T)$ in measured region cannot be fitted using two-band model, which is different from FePn-1111 and FeAs-122 materials⁶-8. Experiments in higher field and lower temperature are needed in order to shed more light on the upper critical field behavior for both magnetic field directions.

There is uncertainty in estimated anisotropy ratio, connected with the uncertainty in determining the upper critical field values from resistivity. This can be solved to some extent by the measurements of angular-dependent resistivity $\rho_{ab}(\theta,\mu_0H)$. Fig. 5 (a) and (b) shows the angular-dependent resistivity for S-99 at 20 K and S-104 at 17 K, respectively. All curves have common cup-like shape and the minimum value at $\theta=90^\circ$, where θ is the angle between the direction of external filed and the c axis. This indicates that the upper critical field along the ab plane is larger than along the c axis for both samples. According to the anisotropic GL model, the effective upper critical field $H_{c2}^{GL}(\theta)$ can be represented as $H_{c2}^{GL}(\theta)$

$$\mu_0 H_{c2}^{GL}(\theta) = \mu_0 H_{c2,ab} / (\sin^2 \theta + \Gamma^2 \cos^2 \theta)^{1/2}$$
 (3)

where
$$\Gamma = H_{c2,ab}/H_{c2,c} = (m_c/m_{ab})^{1/2} = \xi_{ab}/\xi_c$$
.

Since the resistivity in the mixed state depends on the effective field $H/H_{c2}^{GL}(\theta)$, the resistivity can be scaled with $H/H_{c2}^{GL}(\theta)$ and should collapse onto one curve in different magnetic fields at a certain temperature when a proper $\Gamma(T)$ value is chosen³³. Fig. 6 shows the relation between resistivity and scaling field $\mu_0 H_s = \mu_0 H(\sin^2 \theta + \Gamma^2 \cos^2 \theta)^{1/2}$. It can be seen that by adjusting $\Gamma(T)$, a good scaling behavior for S-99 and S-104 can be obtained. The determined $\Gamma(T)$ are shown in the insets of fig. 6(a) and (b). The values are similar to those obtained from fig. 3. But because only one fitting parameter $\Gamma(T)$ can be adjusted for scaling at each temperature, the obtained

		$T_{c,onset}(\mu_0 H = 0)$	$-d(\mu_0 H_{c2})/dT _{T=T_c}$	$H_{c2}(0)$	$\Gamma(0)(=H_{c2,ab}/H_{c2,c})$	$\xi_{ab}(0)$	$\xi_c(0)$
		(K)	(T/K)	(T)		(nm)	(nm)
S-99	$H\ ab$	23.5(1)	2.74(7)	44.69	4.25	5.60	1.32

TABLE I. Superconducting parameters of S-99 and S-104 single crystals.

		$T_{c,onset}(\mu_0 H = 0)$	$-d(\mu_0 H_{c2})/dT _{T=T_c}$	$H_{c2}(0)$	$\Gamma(0)(=H_{c2,ab}/H_{c2,c})$	$\xi_{ab}(0)$	$\xi_c(0)$
		(K)	(T/K)	(T)		(nm)	(nm)
S-99	$H\ ab$	23.5(1)	2.74(7)	44.69	4.25	5.60	1.32
	$H\ c$	23.4(1)	0.649(7)	10.51			
S-104	H∥ab	18.0(2)	3.15(4)	39.22	6.34	7.29	1.15
	$H \parallel_{\mathbf{C}}$	17 9(1)	0.499(4)	6.19			

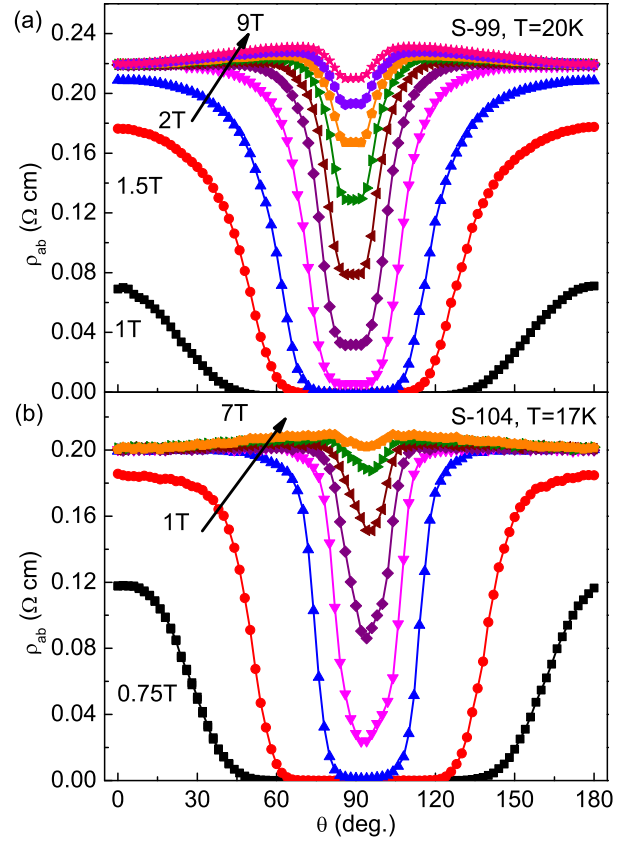


FIG. 5. Angular dependence of $\rho_{ab}(\theta, \mu_0 H)$ for (a) S-99 at 20 K with $\mu_0 H = 1, 1.5, 2, 3, 4, 5, 6, 7, 8, \text{ and } 9 \text{ T} \text{ and (b) S-104}$ at 17 K with $\mu_0 H = 0.75$, 1, 2, 3, 4, 5, 6, and 7 T.

value of $\Gamma(T)$ is more reliable than that determined from the ratio of $\mu_0 H_{c2,ab}(T)$ to $\mu_0 H_{c2,c}(T)$ (which may be influenced by difference among onset, middle and zero resistivity as well as possible misalignment of field). For both crystals, the $\Gamma(T)$ determined for GL theory exhibits the same trend. Anisotropy increases with decreasing temperature from 22 K to 21 K for S-99 and from 17 K to 16 K for S-104 and then almost unchanged (as shown in the insets of Fig. 6 (a) and (b)). The similar behavior is also observed in pure $K_x \text{Fe}_{2-y} \text{Se}_2^{21}$. It should be noted that the anisotropy increases with S doping. It changes from ~ 3 for pure $K_x \text{Fe}_{2-y} \text{Se}_2$ to ~ 6 for S-104^{14,15,20,21}. The larger anisotropy with increasing S content may suggest that two dimensional Fermi surface is becoming less warped with S doping 17 .

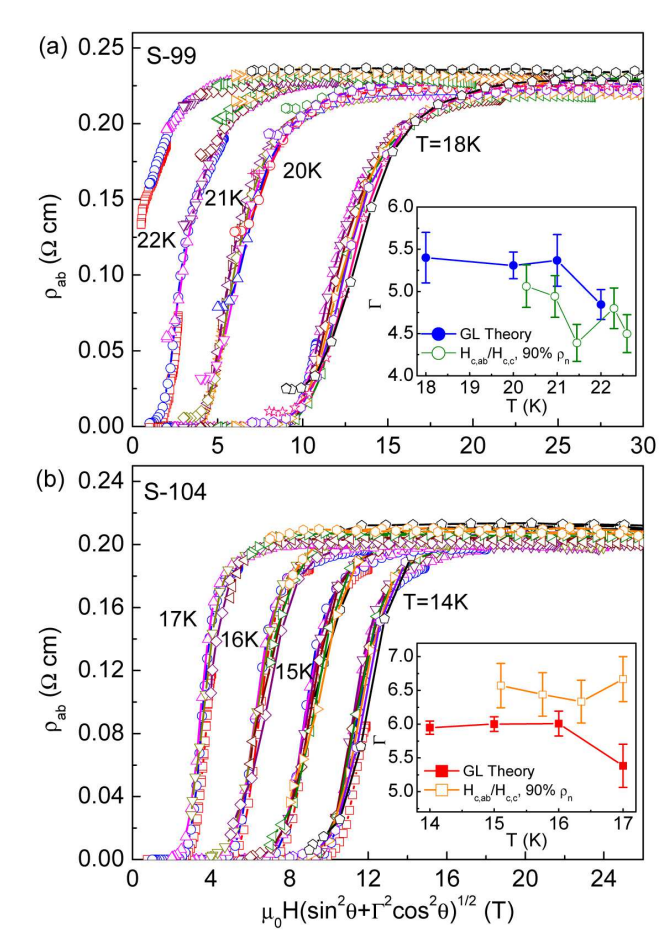


FIG. 6. Scaling behavior of the resistivity versus $\mu_0 H_s =$ $\mu_0 H(\cos^2 \theta + \Gamma^2 \sin^2 \theta)^{1/2}$ for (a) S-99 and (b) S-104 at different magnetic fields and temperatures. The inset (a) and (b) show the temperature dependence of $\Gamma(T)$ determined using GL theory and from fig. 3 for S-99 and S-104, respectively.

CONCLUSION

In conclusion, we have investigated the upper critical fields of $K_{0.70(7)} Fe_{1.55(7)} Se_{1.01(2)} S_{0.99(2)}$ and $K_{0.76(5)}Fe_{1.61(5)}Se_{0.96(4)}S_{1.04(5)}$ single crystals. When compared to pure $K_x \text{Fe}_{2-y} \text{Se}_2$, it is found that the $\mu_0 H_{c2}(T)$ decreases with the increase S content for both field directions. Moreover, the temperature dependence of $\mu_0 H_{c2,c}(T)$ indicates that spin-paramagnetic effect and spin-orbital interaction could be negligible for $H\|c$. On the other hand, it is found that angular-dependence of resistivity $\rho_{ab}(\theta, H)$ follows a scaling law based on the anisotropic GL theory. The values of mass tensor anisotropy $\Gamma(T)$ increase with increasing S content.

V. ACKNOWLEDGEMENTS

We thank John Warren for help with scanning electron microscopy measurements. Work at Brookhaven is supported by the U.S. DOE under Contract No. DE-AC02-98CH10886 and in part by the Center for Emergent Superconductivity, an Energy Frontier Research Center funded by the U.S. DOE, Office for Basic Energy Science.

- Y. Kamihara, T. Watanabe, M. Hirano, and H. Hosono, J. Am. Chem. Soc. **130**, 3296 (2008).
- ² M. Rotter, M. Tegel, and D. Johrendt, Phys. Rev. Lett. 101, 107006 (2008).
- ³ X. C. Wang, Q. Q. Liu, Y. X. Lv, W. B. Gao, L. X. Yang, R. C. Yu, F. Y. Li ,and C. Q. Jin, Solid State Commun. 148, 538 (2008).
- ⁴ F. C. Hsu, J. Y. Luo, K. W. Yeh, T. K. Chen, T. W. Huang, P. M. Wu, Y. C. Lee, Y. L. Huang, Y. Y. Chu, D. C. Yan, and M. K. Wu, Proc. Natl. Acad. Sci. USA **105**, 14262 (2008).
- ⁵ I. I. Mazin, D. J. Singh, M. D. Johannes, and M. H. Du, Phys. Rev. Lett. **101**, 057003 (2008).
- ⁶ F. Hunte, J. Jaroszynski, A. Gurevich, D. C. Larbalestier, R. Jin, A. S. Sefat, M. A. McGuire, B. C. Sales, D. K. Christen, and D. Mandrus, Nature 453, 903 (2008).
- J. Jaroszynski, F. Hunte, L. Balicas, Y.-J. Jo, I. Raičević, A. Gurevich, D. C. Larbalestier, F. F. Balakirev, L. Fang, P. Cheng, Y. Jia, and H. H. Wen, Phys. Rev. B 78, 174523 (2008).
- ⁸ S. A. Baily, Y. Kohama, H. Hiramatsu, B. Maiorov, F. F. Balakirev, M. Hirano, and H. Hosono, Phys. Rev. Lett. **102**, 117004 (2009).
- ⁹ H. C. Lei, R. W. Hu, E. S. Choi, J. B. Warren, and C. Petrovic, Phys. Rev. B 81, 094518 (2010).
- ¹⁰ H. C. Lei, R. W. Hu, E. S. Choi, J. B. Warren, and C. Petrovic, Phys. Rev. B 81, 184522 (2010).
- G. Fuchs, S.-L. Drechsler, N. Kozlova, G. Behr, A. Köhler, J. Werner, K. Nenkov, C. Hess, R. Klingeler, J. E. Hamann-Borrero, A. Kondrat, M. Grobosch, A. Narduzzo, M. Knupfer, J. Freudenberger, B. Büchner, and L. Schultz, Phys. Rev. Lett. 101, 237003 (2008).
- ¹² T. Kida, T. Matsunaga, M. Hagiwara, Y. Mizuguchi, Y. Takano, and K. Kindo, J. Phys. Soc. Jpn 78, 113701 (2009).
- ¹³ J. Guo, S. Jin, G. Wang, S. Wang, K. Zhu, T. Zhou, M. He, and X. Chen, Phys. Rev. B 82, 180520(R) (2010).
- Y. Mizuguchi, H. Takeya, Y. Kawasaki, T. Ozaki, S. Tsuda, T. Yamaguchi, and Y. Takano, Appl. Phys. Lett. 98, 042511 (2011).
- ¹⁵ J. J. Ying, X. F. Wang, X. G. Luo, A. F. Wang, M. Zhang, Y. J. Yan, Z. J. Xiang, R. H. Liu, P. Cheng, G. J. Ye, and X. H. Chen, Phys. Rev. B 83, 212502 (2010)..
- A. F. Wang, J. J. Ying, Y. J. Yan, R. H. Liu, X. G. Luo, Z. Y. Li, X. F. Wang, M. Zhang, G. J. Ye, P. Cheng, Z.

- J. Xiang, and X. H. Chen, Phys. Rev. B **83**, 060512(R) (2011).
- ¹⁷ C.-H. Li, B. Shen, F. Han, X. Y. Zhu, and H.-H. Wen, Phys. Rev. B 83, 184521 (2011).
- ¹⁸ A. Krzton-Maziopa, Z. Shermadini, E. Pomjakushina, V. Pomjakushin, M. Bendele, A. Amato, R. Khasanov, H. Luetkens, and K. Conder, J. Phys.: Condens. Matter 23, 052203 (2011).
- ¹⁹ M. H. Fang, H. D. Wang, C. H. Dong, Z. J. Li, C. M. Feng, J. Chen, H. Q. Yuan, EPL **94**, 27009 (2011).
- ²⁰ D. M. Wang, J. B. He, T.-L. Xia, and G. F. Chen, Phys. Rev. B 83, 132502 (2011).
- ²¹ E. D. Mun, M. M. Altarawneh, C. H. Mielke, V. S. Zapf, R. Hu, S. L. Bud'ko, and P. C. Canfield, Phys. Rev. B 83, 100514(R) (2011).
- $^{22}\,$ H. C. Lei and C. Petrovic, Phys. Rev. B $\pmb{83},$ 180503 (2011).
- ²³ H. C. Lei, M. Abeykoon, E. S. Bozin, K. F. Wang, J. B. Warren, and C. Petrovic, Phys. Rev. Lett. **107**, 137002 (2011).
- ²⁴ H.-S. Lee, M. Bartkowiak, J.-H. Park, J.-Y. Lee, J.-Y. Kim, N.-H. Sung, B. K. Cho, C.-U. Jung, J. S. Kim, and H.-J. Lee, Phys. Rev. B 80, 144512 (2009).
- J. Karpinski, N. D. Zhigadlo, S. Katrych, Z. Bukowski, P. Moll, S. Weyeneth, H. Keller, R. Puzniak, M. Tortello, D. Daghero, R. Gonnelli, I. Maggio-Aprile, Y. Fasano, Ø. Fischer, K. Rogacki, and B. Batlogg, Physica C 469, 370 (2009).
- ²⁶ Z.-S. Wang, H.-Q. Luo, C. Ren, and H.-H. Wen, Phys. Rev. B 78, 140501(R) (2008).
- ²⁷ Z. Bukowski, S. Weyeneth, R. Puzniak, P. Moll, S. Katrych, N. D. Zhigadlo, J. Karpinski, H. Keller, and B. Batlogg, Phys. Rev. B **79**, 104521 (2009).
- ²⁸ D. E. Prober, R. E. Schwall, and M. R. Beasley, Phys. Rev. B 21, 2717 (1980).
- ²⁹ N. R. Werthamer, E. Helfand, and P. C. Hohenberg, Phys. Rev. **147**, 295 (1966).
- ³⁰ T. P. Orlando, E. J. McNiff, Jr., S. Foner, and M. R. Beasley, Phys. Rev. B 19, 4545 (1979).
- ³¹ P. B. Allen, in Handbook of Superconductivity, edited by C. P. Poole, Jr. (Academic Press, New York, 1999) p. 478.
- ³² G. Blatter, M. V. Feigel'man, V. B. Geshkenbein, A. I. Larkin, and V. M. Vinokur, Rev. Mod. Phys. 66, 1325 (1994).
- ³³ G. Blatter, V. B. Geshkenbein, and A. I. Larkin, Phys. Rev. Lett. **68**, 875 (1992).